In presenting the dissertation as a partial fulfillment of the requirements for an advanced degree from the Georgia Institute of Technology, I agree that the Library of the Institution shall make it available for inspection and circulation in accordance with its regulations governing materials of this type. I agree that permission to copy from, or to publish from, this dissertation may be granted by the professor under whose direction it was written, or, in his absence, by the Dean of the Graduate Division when such copying or publication is solely for scholarly purposes and does not involve potential financial gain. It is understood that any copying from, or publication of, this dissertation which involves potential financial gain will not be allowed without written permission.

James Blaire Trimble

UNSTEADY FLOW IN A SMOOTH PIPE AFTER INSTANTANEOUS OPENING OF A DOWNSTREAM VALVE

Part II. Transition from Laminar to Turbulent Flow

A THESIS

Presented to

the Faculty of the

Georgia Institute of Technology

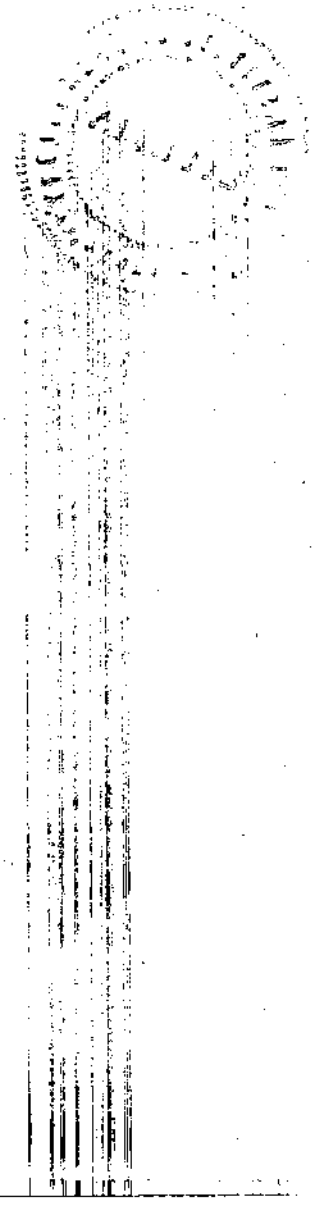

In Partial Fulfillment
of the Degree of
Master of Science in Civil Engineering

by

James Blaire Trimble

August 1955

3 ✓
12 R

UNSTEADY FLOW IN A SMOOTH PIPE AFTER INSTANTANEOUS OPENING OF A DOWNSTREAM VALVE

Part II. Transition from Laminar to Turbulent Flow

Approved: _____

_____

_____

_____

Date Approved by Chairman: Dec. 22, 1955

ACKNOWLEDGMENTS

The writer is appreciative of the assistance of many persons who made this thesis possible. Dr. M. R. Carstens conceived the study and guided the work from the beginning to the end. The extensive experimental program was made possible by a grant from the National Science Foundation. The members of the thesis reading committee were Professor M. R. Carstens, Professor C. E. Kindsvater, and Professor W. R. Metcalfe. The writer is indebted to Mr. E. R. Flynt of the Engineering Experiment Station staff for his assistance with the electronic equipment. Particular acknowledgement is extended to Mr. B. G. Christopher who was a partner in every way during the experimental program. Mrs. Martha McCalla typed the manuscript.

TABLE OF CONTENTS

LIST OF FIGURES

SUMMARY

An experimental study was performed in order to determine the mean flow characteristics in a pipe during flow establishment. The smooth straight circular pipe was horizontally aligned. The upstream extremity of this pipe was a well-rounded inlet which was located in a large reservoir. The downstream extremity of this pipe was unobstructed so that a liquid jet was formed in the atmosphere downstream from the pipe. The flow was established by rapid (effectively instantaneous) release of a disk valve placed against the square-edged downstream end of the pipe. Velocity-time data were obtained from a motion picture record of the jet. Pressure-time data were obtained at selected points along the pipe. These data were recorded by sending the output signals of pressure transducers through an oscillograph.

The experiments were performed with a systematic variation of the independent dimensionless variables. These independent dimensionless variables were pipe length to pipe diameter ratio L/D and an inertial reaction to viscous shear force ratio $gh_oD^3/L\nu^2$. h_o is the piezometric head in the reservoir and ν is the kinematic viscosity of the fluid. The value of L/D was established at 95, 190, 285, 380, and 475. The value of $gh_oD^3/L\nu^2$ was established at $6(10^6)$, $12(10^6)$, $18(10^6)$, $24(10^6)$, and $30(10^6)$. Thus the total number of runs was twenty-five. The velocity-time data are presented in Part I and the pressure-time data are to be presented in Part III.

This portion of the study (Part II) is concerned with the transition from laminar to turbulent flow during flow establishment. Prior to release of the downstream valve, the fluid is at rest in the pipe. For a short time interval following the valve opening, the flow is laminar throughout the pipe. At a later time, the flow becomes unstable at a point and a turbulent spot or region exists. This turbulent region continues to enlarge until the entire pipe is filled with turbulently flowing fluid. A study was made of the time of turbulence inception, of the rate of growth of the turbulent region, and of the position of turbulence inception.

For all runs, the time of turbulence inception was found to be a function of the boundary-layer Reynolds number. Laminar instability appeared when the magnitude of the boundary-layer Reynolds number was approximately 5500. The boundary-layer Reynolds number is based upon the freestream velocity and the nominal boundary-layer thickness. The magnitude of the acceleration or the boundary-layer thickness per se appeared to be of no consequence in establishing the laminar instability.

The rate of growth of the turbulent region was distinctly different in the downstream direction than in the upstream direction. The downstream growth of the turbulent region was approximately 1.35 times the mean velocity of the fluid in the pipe. Upstream rate of growth of the turbulent region was erratic. The turbulence is carried downstream by the flowing fluid and thus the downstream growth represents a transport of turbulence which was generated previously in a region further upstream. The upstream growth of the turbulent region is the result of new laminar instability.

The position in the pipe at which the turbulent region was initiated appeared to be random. The position of the first turbulent spot was found to be between 30 and 270 pipe diameters from the inlet.

UNSTEADY FLOW IN A SMOOTH PIPE AFTER INSTANTANEOUS OPENING OF A DOWNSTREAM VALVE

Part II. TRANSITION FROM LAMINAR TO TURBULENT FLOW

CHAPTER I

INTRODUCTION

Experimental Program.—An experimental study to determine the mean flow characteristics in a pipe during flow establishment was performed in the Hydraulics Laboratory of the Georgia Institute of Technology. Figure 1 is a schematic drawing of the essential features of the equipment.

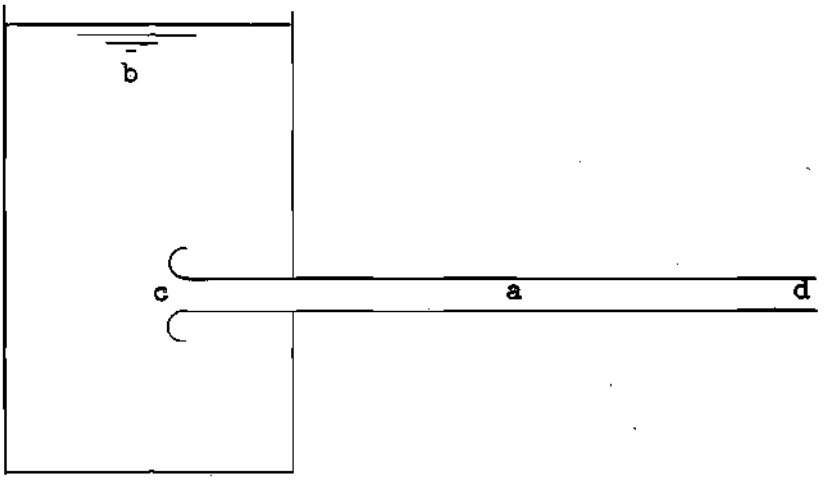

Fig. 1. General Arrangement of the Equipment

A smooth straight circular pipe, a Fig. 1, was horizontally aligned. The upstream extremity of this pipe was a well-rounded inlet at c in a large reservoir b. The downstream extremity of this pipe was unobstructed

so that a liquid jet was formed in the atmosphere downstream from the pipe. The flow was established by rapid (effectively instantaneous) release of a disk valve placed against the square-edged downstream end of the pipe at d. Velocity-time data were obtained from a motion-picture record of the jet. Pressure-time data were obtained at selected points along the pipe. These data were recorded by sending the output signals of pressure transducers through an oscillograph.

The experiments were performed with a systematic variation of the independent dimensionless variables.

$$\frac{V}{\sqrt{2gh_o}} = \phi \left[\frac{t\sqrt{gh_o}}{L}, \frac{L}{D}, \frac{gh_o D^3}{\nu^2 L} \right]$$

and

$$\frac{h}{h_o} = \phi \left[\frac{t\sqrt{gh_o}}{L}, \frac{L}{D}, \frac{gh_o D^3}{\nu^2 L} \right]$$

The letter symbols are defined as follows:

D - inside diameter of the pipe ;

g - acceleration of gravity ;

h - piezometric head in the pipe ;

h_o - piezometric head in the reservoir ;

L - length of pipe ;

ν - kinematic viscosity of the fluid ;

t - time since valve opening ; and

V - mean velocity in the pipe.

The experimental results are reported in other parts[1] of this same study.

Objective of Part II. of this Study.--The magnitude of the velocity in the pipe is increased with time after the instant of valve opening. At the instant of valve opening, the velocity magnitude is zero. As a result of the unbalanced forces on the fluid after the valve is opened, the fluid is accelerated. The velocity magnitude continues to increase until equilibrium is established between the pressure force on the fluid and the shear force.

However, during the process of flow establishment, the flow regime undergoes a radical transformation. In the initial stages or with small values of the velocity, the flow is laminar throughout the pipe. As the velocity magnitude increases a point is reached at which this laminar flow becomes unstable and the laminar flow is replaced by turbulent flow. From the velocity-time and pressure-time records a detailed examination of the laminar-turbulent flow transition is possible. The objective of this thesis (Part II. of the complete study) is to study the time and place of turbulence inception as well as the manner of turbulence growth during flow establishment in a pipe.

Laminar-Turbulent Flow Transition Studies.--There are two general conceptions about the cause of the transition from laminar to turbulent flow. The first is that the flow is made turbulent by external disturbances. These disturbances are usually visualized as being in the free

---

[1]The velocity-time data are contained in Part I. "Mean Flow Characteristics-Velocity" by B. G. Christopher. The pressure-time data are to be contained in Part III. "Mean Flow Characteristics-Pressure and Boundary Shear" by J. E. Roller.

stream outside the boundary layer. The laminar-turbulent flow transition studies of Reynolds, Schiller, and Taylor were based upon this concept. The second concept about the cause of the transition is that the transition is the result of an internal instability of the flow. According to this concept, the initial instability would be within the laminar boundary layer. Tollmein was the first to theoretically determine the conditions for which the flow would be internally unstable. Later Schlichting and Lin refined and extended the theoretical analysis for this type of transition.

The following summary of the laminar-turbulent flow transition studies is taken from Prandtl and Tietjens [1], Dryden [2], and Schlichting [3]. All of these references include an extensive bibliography.

Hagan, in his first famous work with laminar motion in cylindrical tubes, observed that laminar motion ceases to exist when the velocity is increased beyond a certain limit. In a second article, published in 1854, Hagan proved that the laminar-turbulent flow transition not only depends upon the velocity, but also upon the fluid viscosity. Still later, he observed that the transition condition is also function of the diameter of the tube.

In 1883, Osborne Reynolds deduced from dimensional considerations that the transition is a function of the Reynolds number ($R = VD/\nu$). Reynolds' theory was that there existed a certain critical value of the Reynolds number R_c at which turbulence always started. For values of R above the critical value, the flow would always be turbulent, and for values below, the flow would always be laminar. From experiments conducted on two tubes, Reynolds found a complete verification of his ideas and determined the critical value in a pipe to be around 2,100.

However, the simplicity of Reynolds' investigation ignored the possibility of the critical value varying with the experimental apparatus. With a different experimental setup, Reynolds repeated his experiments and determined the critical value to be 12,000-14,000. In the first investigation, Reynolds had merely connected his circular tube to the water faucet. But in his second, the water flowing from the faucet was first allowed to come to rest in a large reservoir and entered the pipe through a well rounded entrance. The difference seemed obviously to be in the degree of initial turbulence present. The expectation was that the critical Reynolds number could be made much higher by minimizing the initial disturbances. This has been shown to be true by subsequent investigators. Barnes and Coker, reported a value of 20,000. Ekman conducted experiments with the purpose of obtaining as high a value for R_c as possible. He reported critical Reynolds numbers up to 50,000.

Reynolds' original value for R_c was determined under conditions with extreme initial turbulence. A more recent interpretation of Reynolds' earlier work is that for values of R less than 2,100, the flow is always laminar. Utilizing this interpretation, the lower critical Reynolds number in a pipe is accepted as 2,100. The existence of a definite upper critical Reynolds number, one above which the flow will always be turbulent, is disputed.

In 1938, Taylor presented a theory in which the free-stream turbulence was the principal factor causing the transition. He assumed that the transition was the result of separation in regions of adverse pressure gradients. This assumption led to the conclusion that the critical Reynolds number was a function of the intensity of free-stream turbulence.

In contrast to Taylor's theory, was the alternative view that the transition was the result of instability of the laminar boundary layer in which minute disturbances grew exponentially. About 1929, Tollmien attempted to determine theoretically the necessary conditions in order for disturbances, in the form of velocity variations, to increase with time. For this investigation, he assumed a boundary layer of constant thickness near a flat plate without pressure gradient. The velocity distribution within the boundary layer was taken to be that computed by Blasius. Tollmien's calculations indicated that only disturbances in a certain range of frequencies would increase with time, and then, only if the boundary-layer Reynolds number was greater than a certain critical value.

Almost immediately, groups began searching for experimental confirmation of Tollmien's theory. However, experiments at the National Bureau of Standards, California Institute of Technology, Massachusetts Institute of Technology, and Cambridge University, all failed to show any signs of the amplified disturbances.

In 1940, Schubauer and Skramstad of the National Bureau of Standards, were engaged in the study of transition with a flat plate and with extremely low turbulence levels. They obtained records of the velocity fluctuations in the boundary layer by means of a hot wire anemometer. The unexpected result was that the frequency of the oscillations agreed with that predicted by Tollmien.

Dryden explained the reason this phenomena had not been previously observed. In all previous investigations, the stream turbulence had been much greater than in the Schubauer and Skramstad experiments. The

internal boundary-layer oscillations were impossible to identify because of the superimposed irregular fluctuations of the free-stream turbulence. Under these conditions, the transition was controlled by the free-stream turbulence in accordance with Taylor's theory.

Schlichting, in 1935, extended Tollmien's calculations to include boundary-layer flows with pressure increase and pressure decrease. His results predicted a lower critical boundary-layer Reynolds number for decelerated flow than that for plate flow, and a higher critical boundary-layer Reynolds number for accelerated flow.

The latest theoretical contribution to Tollmien's theory was made by Lin. He undertook a revision of the mathematical theory of the stability of parallel laminar flow and clarified some features of Tollmien and Schlichting's calculations which had been criticized. Lin's results varied only slightly with those of Schlichting's.

Thus the present ideas of laminar-turbulent flow transition may be stated as follows. If the free-stream or external disturbances are less than a limiting magnitude, the transition is the result of internal instability of the laminar boundary layer. Conversely if the free stream or external disturbances are greater than this limiting magnitude, then the transition is the result of these external disturbances. No quantitative information is available concerning the limiting magnitude of the external disturbances.

CHAPTER II

TIME SEQUENCE OF EVENTS IN FLOW ESTABLISHMENT

The time sequence of events which occur during flow establishment can be reconstructed by reference to the pressure-time and velocity-time records. For purposes of illustration the data of Run No. 29 has been selected.

On Fig. 2 is shown the value of the dimensionless piezometric head h/h_o, at equally spaced stations along the pipe, as a function of the dimensionless time $t\sqrt{gh_o}/L$. The values of the controlled experimental parameters for Run No. 29 were $gh_oD^3/L\upsilon^2 = 30 \times 10^6$ and $L/D = 475$. The values of the piezometric head were determined from pressure transducer records[1] at the stations which were 94, 189, 284, and 379 pipe diameters from the pipe inlet. The pressure is atmospheric at the outlet, $x/D = 475$, after the valve is opened, hence the piezometric head is zero for $t \geqslant 0$. The piezometric head at the inlet, $x/D = 0$, has been computed from velocity-time data from the relationship[2]

$$\frac{h}{h_o} = 1 - \frac{V^2}{2gh_o} - \frac{D}{\sqrt{8}\sqrt{gh_o}} \frac{dV}{dt} \qquad (1)$$

For Run No. 29 the minimum value of the third term of the right side of Eq. (1) is 0.00073. Since this is small in relation to unity, the term

---

[1] A complete description of the equipment and technique of determining pressure is contained in Part I. "Mean Flow Characteristics-Velocity", by B. G. Christopher which is a part of this study. The complete presentation of pressure-time data is to be contained in Part III. "Mean Flow Characteristics-Pressure and Boundary Shear", by J. E. Roller.

[2] The derivation of this relationship is presented in APPENDIX A.

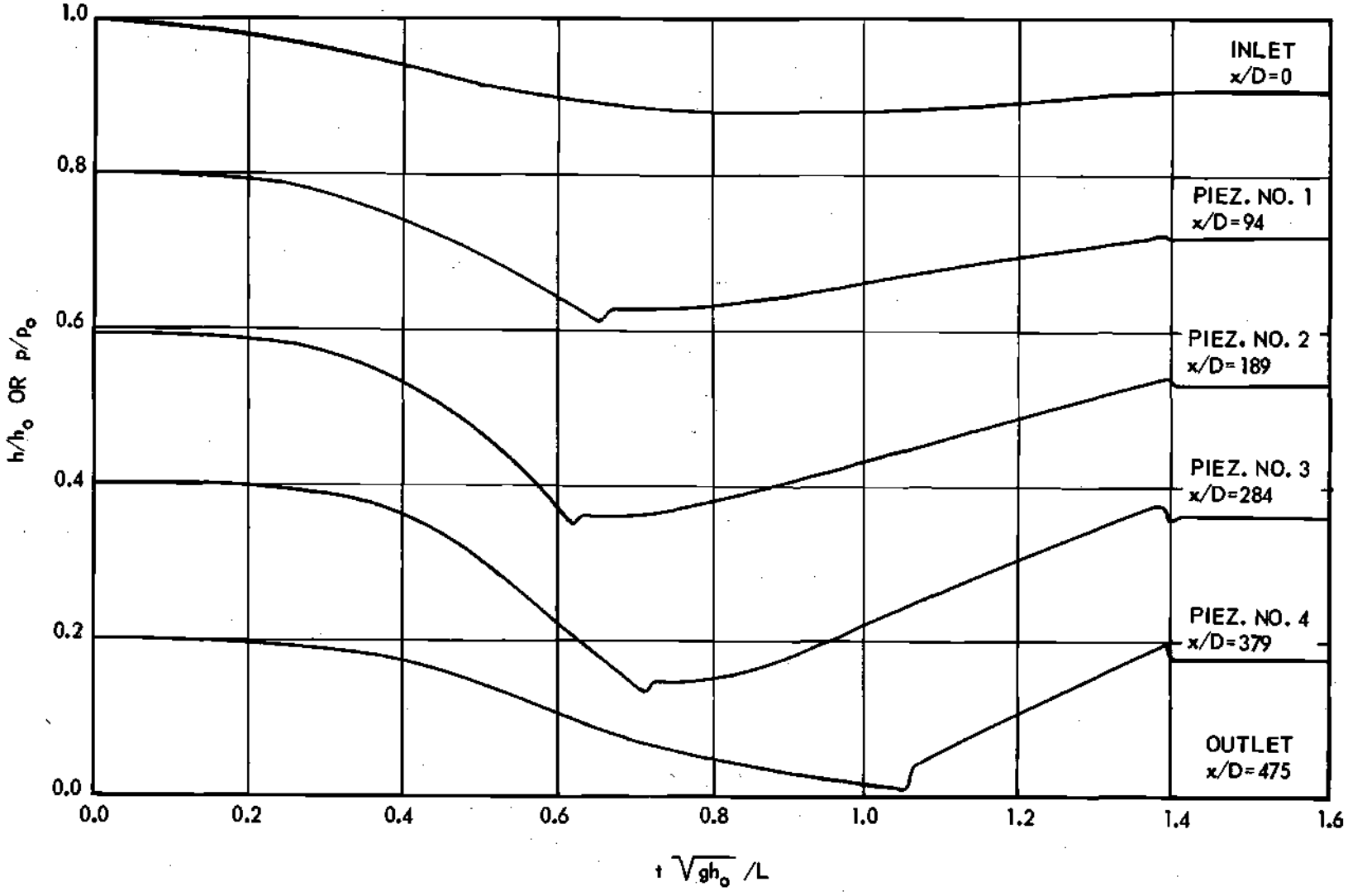

Figure 2. Pressure-time Curves of Run No. 29.

may be neglected. Therefore, the slope of the h/h_o curve at $x/D = 0$ on Fig. 2 is proportional to $-V\ dV/dt$. A negative slope of this h/h_o curve is associated with a positive value of dV/dt; a zero slope is associated with a zero value of either V or dV/dt; and, a positive slope is associated with a negative value of dV/dt. Thus the fluid was accelerated in the time interval $0 < t\sqrt{gh_o}/L < 0.9$ and was decelerated in the time interval $0.9 < t\sqrt{gh_o}/L < 1.4$.

Figure 3 has been constructed from the data shown on Fig. 2. Figure 3 is simply a plot of the dimensionless hydraulic grade line or piezometric head line at successive equal time increments. Since there were four pressure transducer readings, the computed inlet piezometric head, and the outlet piezometric of zero at all times, the piezometric head lines of Fig. 3 are based upon six values.

The following analysis is based upon the one-dimensional equation of motion as presented in APPENDIX B in addition to the data presented on Figs. 2 and 3.

Prior to the valve opening the fluid is at rest throughout the pipe as well as in the reservoir. Therefore at $t < 0$ the dimensionless piezometric head h/h_o has the constant value of unity at all measuring stations.

At the instant the downstream valve is opened the piezometric head is changed to a zero value at the outlet. At this instant the velocity is zero throughout the pipe. Also the velocity distribution is constant throughout the pipe. Therefore, the piezometric head line will be a straight line varying from h_o at the inlet to zero at the outlet. Since the velocity is zero, the shear force is zero. Thus the motivating force, the piezometric head gradient, is utilized entirely to accelerate the

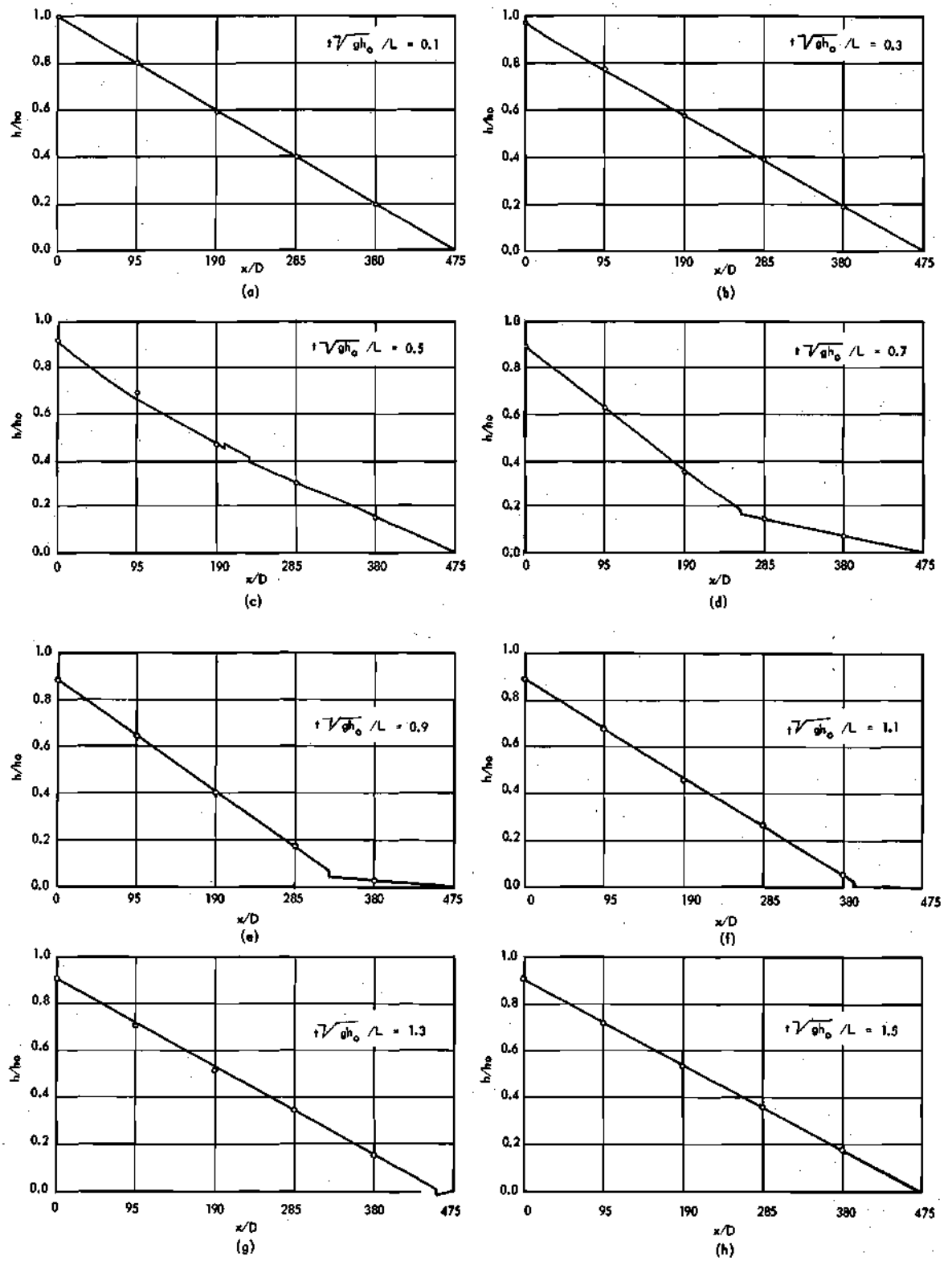

Figure 3. Hydraulic Grade Lines at Successive Times for Run No. 29.

fluid. Therefore, at the instant of valve opening the acceleration is a maximum (approximately 1.0 g for Run No. 29).

Figure 3(a) represents conditions a short time after valve opening when the velocity magnitude is small and the flow is laminar throughout the pipe. Since the velocity is small, the shear force will also be small valued at this time. Only about 7 percent of the motivating force (piezometric head gradient) is utilized in overcoming shear. Therefore the acceleration is only slightly less than the maximum at this instant.

Figure 3(b) represents conditions when the flow is still laminar throughout the pipe but when an appreciable fraction of the motivating force (piezometric head gradient) is utilized to overcome the shear force. Approximately 16 percent of the piezometric head gradient is utilized to overcome the shear force in the region where this gradient is straight. Hence approximately 84 percent of the piezometric head gradient is utilized to accelerate the fluid. The acceleration dV/dt is somewhat less than 84 per cent of the maximum because the gradient is also decreasing with time as the value of h/h_o at $x/D = 0$ decreases. This effect can be clearly seen by drawing a straight line from the point (0, 1) to the point (475, 0) and observing that the plotted gradient is slightly less. Thus the acceleration dV/dt is approximately 79 percent of the initial value.

On Fig. 3(c) is shown the piezometric head line shortly after a turbulent flash or spot has appeared at about 210 pipe diameters from the inlet. The presence of this turbulent flow region is not yet apparent from the pressure transducer records (Fig. 2). The flow is still laminar both upstream and downstream from this turbulent region. The method of

determining the time and position of turbulence inception is discussed in Chapter III.

The laminar flow region downstream from the turbulence ($225 < x/D < 475$) is isolated from the inlet with the result that the velocity distribution is independent of distance from the inlet. Thus the piezometric head line is straight in this downstream laminar region. About 24 percent of the piezometric head gradient is utilized to overcome the shear force in this region and about 75 percent is available to accelerate the fluid. However, since the value of the gradient is considerably less than the initial value, the acceleration dV/dt is only 36 percent of the initial value.

The laminar flow region upstream from the turbulence ($0 < x/D < 200$) is a region of spatially developing velocity profile. Since the piezometric head gradient is steeper in the upstream laminar flow region than in the downstream laminar region, this region must be a region in which K_m is increasing with distance. Also the shear force is likely to be a function of distance from the inlet. The numerical separation of the portion of the local piezometric head gradient to overcome the shear force is not possible from the data in this region.

The turbulent flow region of Fig. 3(c) which is between 200 and 225 pipe diameters from the inlet is another region in which velocity distribution and shear force are independent of position. In other words, the local turbulent diffusion is the same at $x/D = 205$ as at $x/D = 220$. Thus the piezometric head gradient is straight. However, the piezometric head gradient is steeper than in the downstream laminar region because the shear force is greater in the turbulent flow.

In the intermediate time between Figs. 3(c) and 3(d), a piezometric head discontinuity or "pip" is registered at the measuring station $x/D = 94$ and at the measuring station $x/D = 189$. These "pips" are clearly shown on Fig. 2. A "pip" is interpretated as a manifestation of the passage of the laminar-turbulent flow interface past the piezometer. The reason for the rapid change in piezometric head across this interface is that the kinetic energy is greater in the laminar flow than in the turbulent flow even though the mean velocity V is identical both sides of the interface. Figure 4 is a sketch portraying this idea.

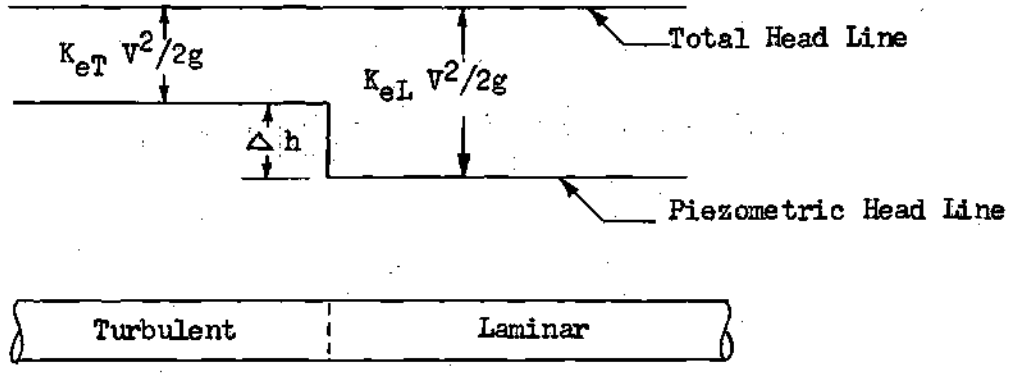

Fig. 4. Piezometric Head Change at the Laminar-Turbulent Flow Interface.

The velocity distribution of turbulent flow is nearly uniform with the result that the kinetic energy correction coefficient K_{eT} is only slightly greater than unity. The velocity distribution of laminar flow is not uniform with the result that K_{eL} is considerably in excess of unity. In fact, for fully developed laminar flow in a pipe K_{eL} is equal to two. Therefore the rapid change in piezometric head is

$$\frac{\Delta h}{h_o} = (K_{eL} - K_{eT}) \frac{V^2}{2gh_o}$$

If the flow is laminar by a piezometer, the piezometric head will rapidly increase as the laminar-turbulent flow interface passes this piezometer. Therefore, the "pip" is a manifestation of the interface but is not indicative as to whether the interface is moving upstream or downstream.

Figure 3(d) represents conditions a short time after the laminar-turbulent interface has passed both the piezometer at $x/D = 94$ and at $x/D = 189$. The flow condition is visualized as being turbulent in the region, $0 < x/D < 255$ and laminar in the region $255 < x/D < 475$. The laminar-turbulent flow interface is moving downstream being at $x/D = 255$ at the time of Fig. 3(d). It is apparent from this interpretation that the rate of growth of the turbulent region is vastly different in the upstream direction than in the downstream direction. The laminar-turbulent interface of the downstream end of the turbulent region is perceived as moving downstream at essentially the mean velocity V. This velocity of movement of the interface may be slightly greater than V as new fluid is entrained from the preceding laminar flow by the turbulent eddies. This concept of turbulence growth is untenable at the upstream end of a turbulent region, since it would follow that turbulence would never spread upstream. The explanation of the turbulence spreading upstream is that new regions of instability occur upstream from the point of initial laminar flow instability. Since the upstream spreading of turbulence is the result of a new phenonemon, the upstream spreading may be erratic.

Figure 3(d) thus represents two well-defined regions of flow, that is, laminar for values of x/D greater than 255 and turbulent for values of x/D less than 255. Since the laminar region has been isolated from

the inlet by the turbulence, the result is that the velocity distribution is independent of the distance from the inlet. Thus the piezometric head line is straight. About 48 percent of the piezometric head gradient is utilized to overcome the shear force in this region and about 52 percent is available to accelerate the fluid. However, since the value of the piezometric head gradient is small in relation to the initial value, the acceleration dV/dt is only 18 percent of the initial value. The turbulent flow region ($x/D < 255$) is likewise a region of straight piezometric head gradient since the velocity distribution is independent of the distance from the inlet. However, in this region approximately 86 percent of the piezometric head gradient is utilized to overcome the shear force. Thus, with the same mean velocity V and acceleration dV/dt, 86 percent of the available piezometric head is utilized to overcome the shear force in turbulent flow as opposed to 48 percent in laminar flow. The disparity between the shear force per unit length in turbulent flow and laminar flow is even greater because of the differences in value of the piezometric head gradient. With the same mean velocity V and acceleration dV/dt, the turbulent shear force per unit length is about 6.7 times the corresponding value for laminar flow.

Figure 3(e) is very similar to Fig. 3(d) in physical interpretation. The laminar-turbulent interface is now about 325 pipe diameters from the inlet. The acceleration dV/dt is negligible. Thus all the available piezometric head gradient is utilized to overcome the shear force in both the laminar and turbulent flow regions. The turbulent shear force per unit length is about 10 times the corresponding value for laminar flow.

Figures 3(f) and 3(g) are similar in physical interpretation to Figs. 3(c) and 3(d). The progressive downstream movement of the laminar-turbulent interface is apparent. The significant difference between the flow conditions at these times and the flow conditions at the earlier times is that the fluid is being decelerated. The inertial reaction is similar to a motivating force in the case of deceleration. Thus the shear force is greater than the piezometric head gradient by the amount of the inertial reaction. This effect is particularly noticeable at the extreme right of Fig. 3(g) where the piezometric head gradient is actually positive in the laminar flow region.

In the intermediate time between Figs. 3(g) and 3(h), turbulent flow reaches the end of the pipe at $x/D = 475$. The exact time that turbulence reaches the end of the pipe is the time that the abrupt piezometric head decreases are shown on Fig. 2. This time for Run No. 29 is when the value of $t\sqrt{gh_o}/L$ is 1.39. The explanation of the abrupt piezometric head decrease at intermediate measuring stations is as follows. The laminar-turbulent interface is moving toward the outlet. Turbulent flow is on the upstream side of the interface and laminar flow is on the downstream side of the interface. Due to the differences in kinetic energy, the piezometric head is greater in the turbulent flow than in the laminar flow. However, the outlet is a station of fixed piezometric head, that is, $h/h_o = 0$ at $x/D = 475$ at all times. Thus as the laminar-turbulent interface reaches the end of the pipe, the piezometric head just behind the interface suddenly decreases by the amount

$$\frac{\Delta h}{h_o} = (K_{eL} - K_{eT}) \frac{V^2}{2gh_o}$$

With this sudden drop in the piezometric head at the outlet, the piezometric head gradient is also suddenly increased since the value of h/h_o at the inlet, $x/D = 0$, remains essentially constant. This sudden pivoting of the piezometric head line about the inlet piezometric head value results in a piezometric head drop at each measuring station. The magnitude of the piezometric head drop is directly proportional to the distance from the inlet. Therefore, the piezometric head decrease at $x/D = 379$ is $(4/5)(\Delta h/h_o)$, at $x/D = 284$ is $(3/5(\Delta h/h_o)$, at $x/D = 189$ is $(2/5)(\Delta h/h_o)$, at $x/D = 94$ is $(1/5)(\Delta h/h_o)$, and at $x/D = 0$ is zero. This progressive effect can be clearly discerned on Fig. 2.

Finally Fig. 3(h) represents the steady state condition. The acceleration dV/dt is zero. The flow is turbulent throughout the pipe. The piezometric head gradient is entirely utilized to overcome the shear force. In concluding the discussion of the time sequence of events during flow establishment, it is interesting to note that the total elapsed time from the time of valve opening to the time of Fig. 3(h) is only 1.31 seconds.

CHAPTER III

RESULTS AND ANALYSIS OF RESULTS

Critical Boundary-Layer Reynolds Number.--Tollmien's theory of boundary-layer instability has received notable support since Schubauer and Skramstad succeeded in obtaining records of spontaneously occurring velocity fluctuations in the boundary-layer which confirmed Tollmien's ideas. According to Dryden, its validity and applicability are beyond question. Small disturbances in the laminar boundary layer of a certain range of frequencies are amplified until they burst into turbulence, provided that the boundary layer Reynolds number R_δ is greater than the minimum critical boundary layer Reynolds number $R_{\delta c}$. The following analysis of the laminar-turbulent transition is based on the supposition that a $R_{\delta c}$ exists.

It should be noted that according to Tollmien's theory, $R_{\delta c}$ is a function of the frequencies of the disturbance. If $R_{\delta c}$ is to be of a constant value, the frequencies of the disturbances must be of a constant value. Therefore, in order to establish a consistent basis for the application of Tollmien's theory, it seems necessary to control the disturbances which may effect the boundary layer stability. If the disturbances were left to chance alone, the likelihood of the transition occurring at a constant value of R_δ would also be a chance occurrence. For this reason, a 1/8-inch band of sand grains were placed inside the rounded inlet just upstream from the point of tangency with the pipe wall. The sand grains were of such size that they passed the No. 100 seive and

were retained on the No. 200 seive. The presumption was that the sand grains would consistently produce disturbances in the boundary layer of a sufficiently wide range of frequencies to allow the boundary layer to become turbulent at the earliest possible time. Thus disturbances arising from sources other than the sand grains, should not effect the transition.

Two preliminary investigations were made to determine the effectiveness of the sand grains. The reservoir was filled, calmed, and then discharged through the pipe. Turbulent flow was established soon after opening the valve. As the head decreased, the flow changed intermititly and then permanently to laminar. Approximately four hours were taken for the head to fall four feet so the deceleration had little effect on the transition. In the first investigation, the inlet contained only the sand grains, but in the second, two wires 0.01 inch in diameter were crossed in front of the inlet. The behavior of the flow was almost identical in the second investigation with that in the first, and in each case, laminar flow first developed at a R of about 16,000. The conclusion was that outside disturbances, at least to the degree of that afforded by the cross wires, would not effect the transition as long as the inlet contained the sand grains. Therefore, the sand grain disturbances should initiate the transition in every case, and hence the boundary layer Reynolds number should be a consistent criterion for determining the transition.

If the assumption is made that the frequencies of the disturbances are no longer a variable affecting $R_{\delta c}$, there seems to be only two other possible variables. Schlichting's computations indicate that $R_{\delta c}$ is dependent on the acceleration, and it seems likely that the boundary

layer thickness δ, or δ/r_o may also effect the transition. Thus,

$$R_{\delta c} = \phi \left[\frac{\delta \, dv_c/dt}{v_c^2} , \frac{\delta}{r_o} \right]$$

The desirable approach to determining the validity of the above relationship is to evaluate each term at the time turbulence originated. However this is impossible since the time of turbulence inception is not known. It was therefore necessary to evaluate the terms at the time that turbulence was first positively detected, which in each case was the first appearance of a pressure "pip" on the pressure time-curves.

The computed R_δ is based on Schiller's velocity profile shown in Fig. 5. The velocity distribution in the boundary layer δ is parabolic and the velocity distribution in the core is constant. The boundary

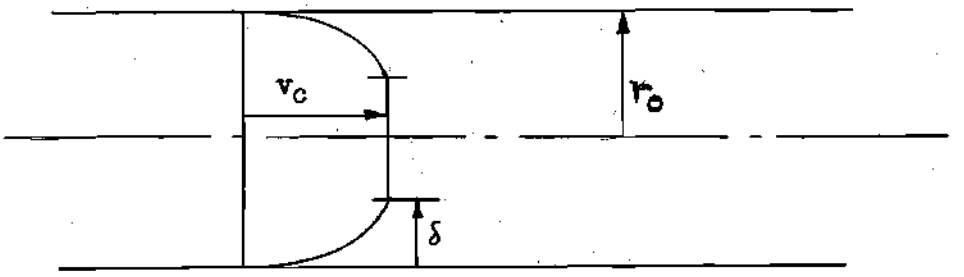

Fig. 5. Schiller's Velocity Profile

layer Reynolds number is $R_\delta = v_c \delta/\nu$. Values of δ, the boundary layer thickness, were determined by several methods using experimental data.[1]

In Figs. 6 and 7 are shown R_δ versus $\delta(dv_c/dt)/v_c^2$ and R_δ versus δ/r_o respectively. The results show the acceleration parameter to be of

---

[1] See Part I of this study "Mean Flow Characteristics-Velocity" by B. G. Christopher.

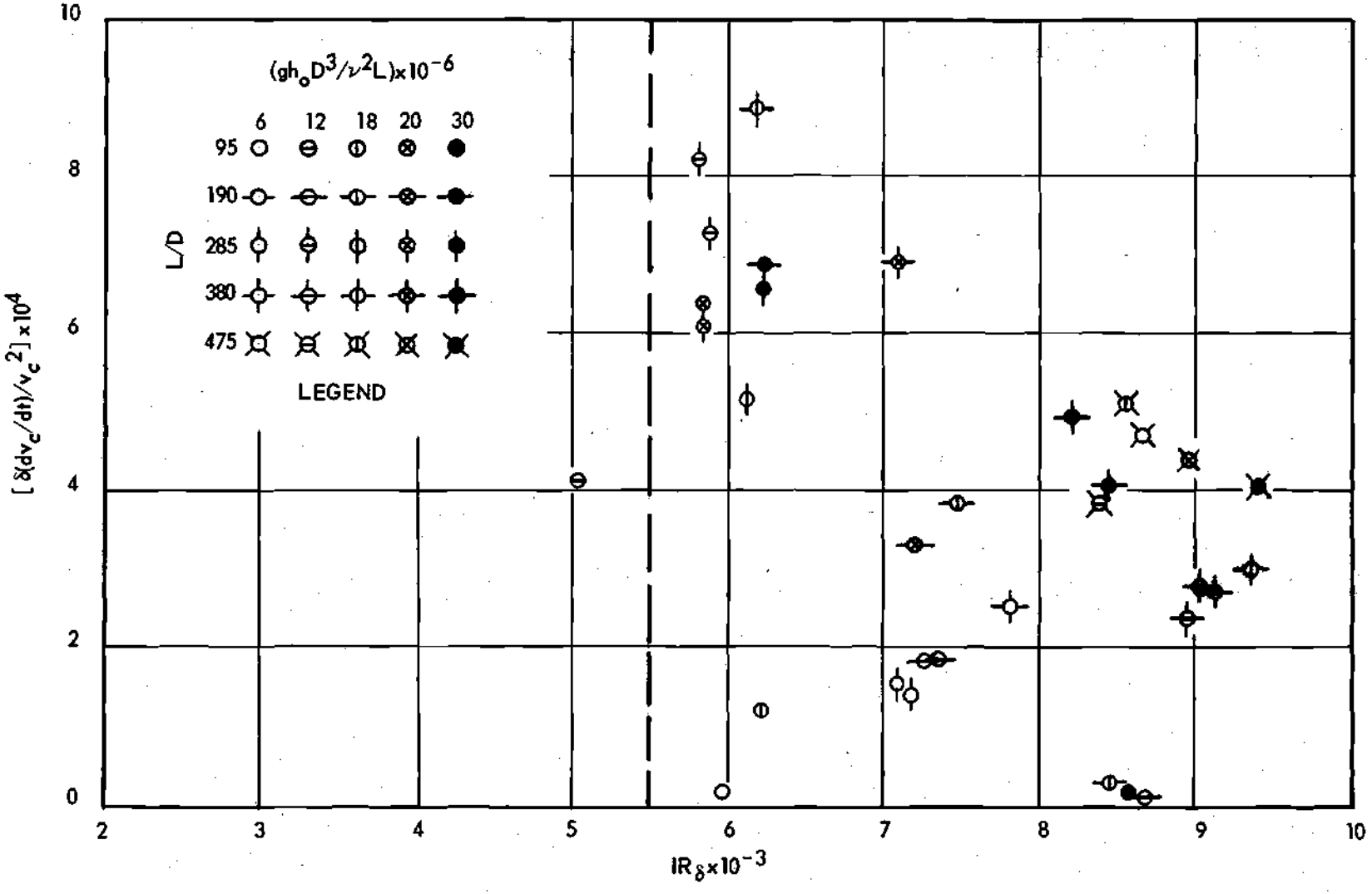

Figure 6. Boundary Layer Reynolds Number Versus Acceleration Parameter at the Time that Turbulence is First Detected.

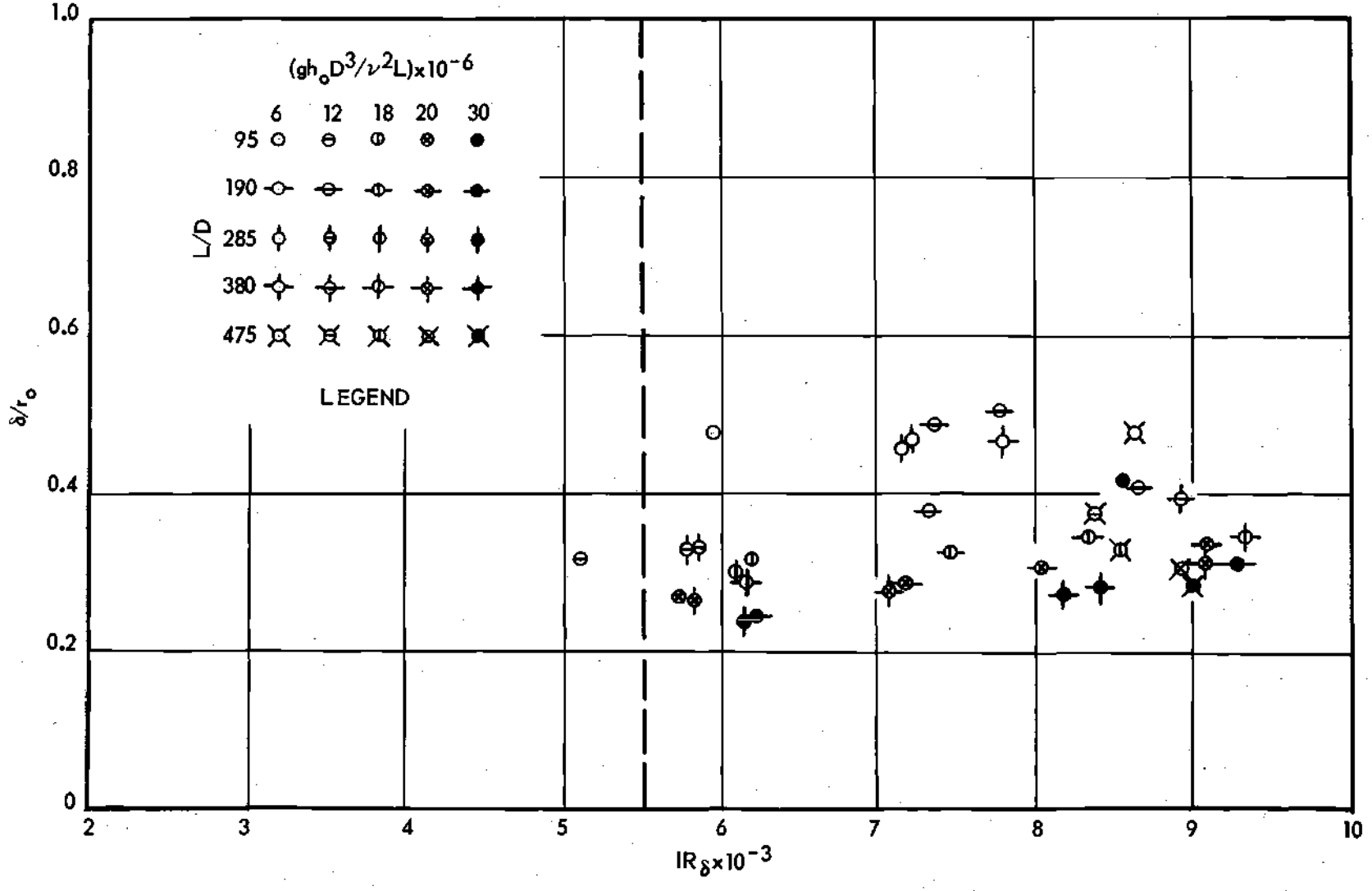

Figure 7. Boundary Layer Reynolds Number Versus Dimensionless Boundary Layer Thickness at the Time that Turbulence is First Detected.

a wide range of values and of no apparent relationship. Values of δ/r_o are concentrated between 0.2 and 0.5 but seem to vary with the head parameter. The transition occurs at the lower values of δ/r_o for higher head parameter runs and at the higher values of δ/r_o for lower head parameter runs. Since the boundary layer thickness δ is primarily a function of time, and since the velocity V is a function of time and the head parameter, the product of V and δ will reach a certain value at an earlier time, and hence at a lower value of δ, in the higher head parameter runs. This trend is indicative of the transition occurring at a constant value of R_δ. Evidently the values of δ/r_o at the time of turbulence inception could be made to extend over a greater range of values by merely extending the range of the head parameter.

It should be emphasized that the boundary layer Reynolds number shown in Figs. 6 and 7 is not $R_{\delta c}$. The variation in R_δ shown may be explained at least partially, by reconsidering the manner (time) in which R_δ is computed. If the point of turbulence inception is at or near a piezometer, the R_δ shown may be expected to be nearly the same as $R_{\delta c}$, for there will be only a short interval of time before the turbulence is detected. But if the point of turbulence inception is some distance from a piezometer, there will be a considerable time lag before the turbulence is detected, and hence the computed R_δ will be greater. A variation in the distance from the points of inception to a piezometer would therefore produce a variation in the computed R_δ. Probably, the distances from the points of turbulence inception to a piezometer vary widely, and hence the minimum R_δ shown should be nearly equal to $R_{\delta c}$. Thus $R_{\delta c}$ seems to be fairly well defined as about 5,500.

This value of $R_{\delta c}$ is considerably higher than the minimum value of 1725 obtained by Tollmien [3] for flow past a flat plate and verified by Schubauer and Skramstad [4]. On the other hand, Goldstein [5] states that values of $R_{\delta c}$ have been measured in the range between 1,650 and 5,750 for flow past a flat plate. This discrepancy as to the numerical magnitude has not been satisfactorily explained. In any event, the value of $R_{\delta c}$ of 5,500 does not seem unreasonable even though the value is close to the upper value quoted by Goldstein. The value of $R_{\delta c}$ for pipe flow would be expected to be somewhat higher than for a flat plate because of the stabilizing effect of confining the flow. Also, it should be noted that the unsteadiness of the flow may account for a high observed value of $R_{\delta c}$. That is, if when R_{δ} reaches a certain critical value the disturbances are assumed to be increased with time until turbulence appears, R_{δ} will be of a greater value at the time of turbulence inception that at the time that the disturbances first began to be amplified. Therefore, the value of R_{δ} at the time the disturbances first began to be amplified will be less than 5,500.

Rather than the magnitude of $R_{\delta c}$, the surprising result is that the value of $R_{\delta c}$ appeared to be independent of the acceleration (Fig. 6). Schlichting [3] has theoretically analyzed the affect of convective acceleration and he found that the value of $R_{\delta c}$ is strongly influenced by the magnitude of the convective acceleration. While it is true that the acceleration of this experiment was local acceleration, an analogous effect was anticipated.

In Fig. 8 are shown the times of turbulence inception. These times were computed by computing the times that R_{δ} reaches a value of 5,500.

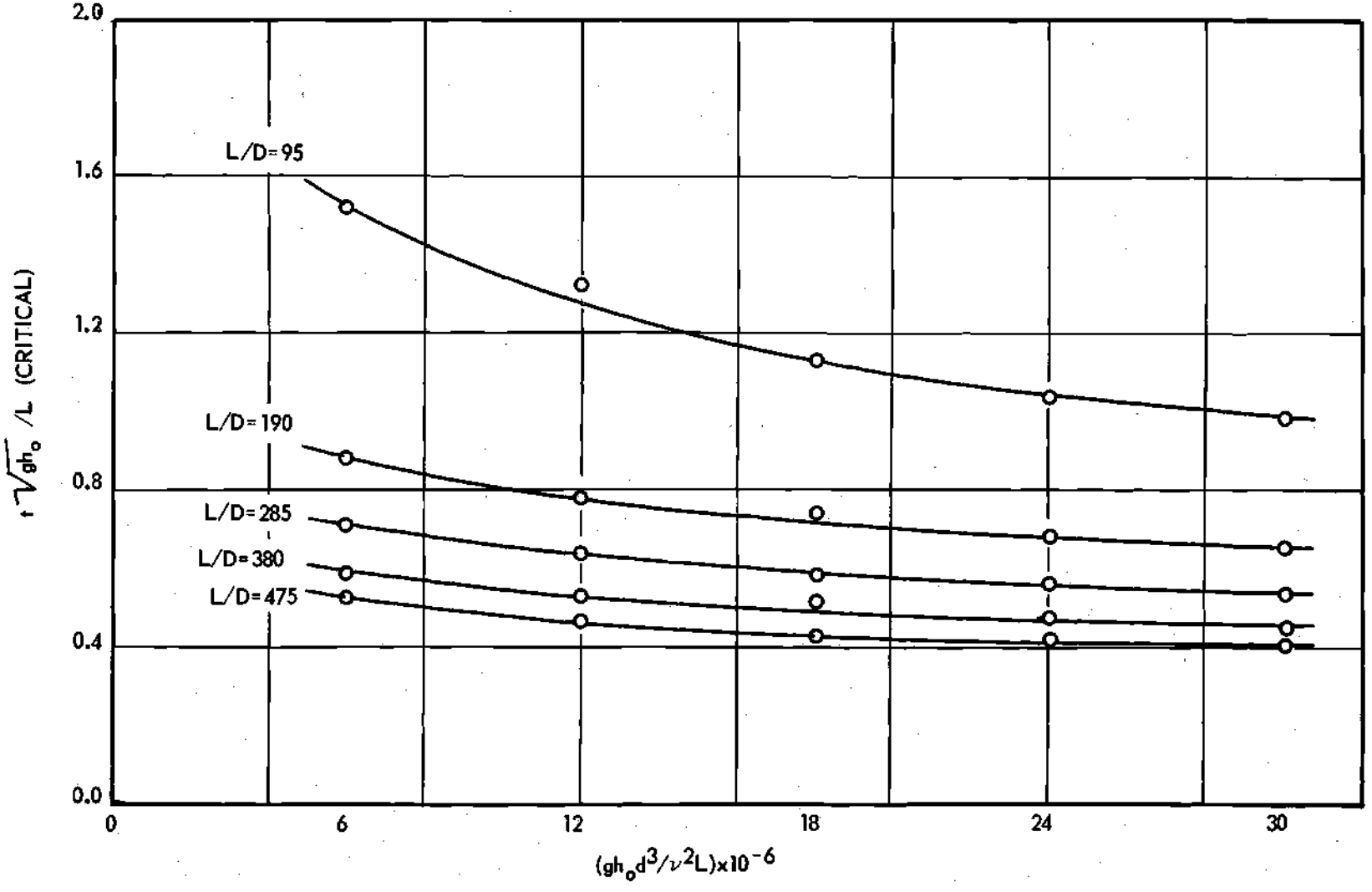

Figure 8. Head Parameter Versus Time of Turbulence Inception.

Rate of Growth of Turbulence.--From the explanation of the pressure-time data and the hydraulic grade lines given in Chapter II, one may conclude that the transition from laminar to turbulent flow throughout the pipe is not an instantaneous occurrence but rather occurs during a finite interval of time. The first appearance of turbulence is credited in the preceding section to boundary layer instability. Once laminar flow has become unstable, new eddies are continually formed upstream as the eddies first formed are swept away downstream. The eddies first formed create disturbances which in turn create new eddies. Thus the downstream interface moves downstream with a velocity equal to the mean velocity of the fluid plus the relative velocity of the interface to the fluid.

The upstream laminar-turbulent interface could conceivably also move upstream due to similar generation of new eddies at the upstream interface. If the velocity of the interface relative to the fluid were the result of new eddy generation at the interface, the relative velocity of both interfaces would be identical in magnitude. Since the fluid is moved downstream with the mean velocity V, the absolute velocity of the downstream interface would be twice the relative velocity greater than the upstream interface velocity. However, the upstream interface is seen in Figs. 4(c) and 4(d) to move upstream much faster than the downstream interface moves downstream. Thus it is concluded that the upstream movement of the turbulence is the result of different physical action than the downstream movement.

A reasonable explanation is that turbulence does not move upstream but that new turbulence is created upstream from the earlier regions of instability. If this hypothesis is correct, the upstream expansion of

the turbulent region is dependent only upon the stability of the laminar boundary layer, whereas the downstream expansion of the turbulent region is primarily dependent upon the mean velocity V which carries the previously generated turbulence in a downstream direction. Since the stability of the laminar boundary layer is dependent upon viscous forces, boundary layer dimensions, boundary layer velocity distribution, as well as free stream velocity; the expectation is that the upstream expansion is difficult to determine and even more difficult to generalize. Also, the origin of turbulence is generally so far upstream that it is not possible to observe the upstream turbulent growth except at one piezometer. For these reasons, the rate of growth of turbulence upstream is not considered.

The time that turbulence reaches each of the piezometers and the outlet is readily obtainable from the pressure-time curves (Fig. 2), as is explained in Chap. II. By utilizing these times and the distances between observation points, the average downstream rate of growth of turbulence V^* between points may be calculated. Thus

$$V^* = \Delta \ell / \Delta t \qquad (2)$$

in which $\Delta \ell$ is the distance between points of observation and Δt is the difference in times at the times turbulence reaches the points of observation. In the table of APPENDIX C are shown the values of the time parameter $t\sqrt{gh_o}/L$ and the velocity parameter $V/\sqrt{2gh_o}$ at the time turbulence reaches each point of observation.

The above concept of V^* pertains only to one interface and may not be used if turbulence originates between the two points of observation. However, at this time, one does not know exactly where turbulence originates, nor is it possible to know positively if the turbulence

approaches the piezometers from the upstream or downstream side. If one assumes that turbulence progresses from its point of origin in a continuous fashion, one may deduce from the pressure-time curves among which three piezometers turbulence originated. For instance, in Fig. 2 the sequence of occurrence of pressure "pips" is piezometers Nos. 2, 1, 3, and 4. Probably, turbulence originated in Run No. 29 between piezometers Nos. 1 and 3. This sequence of pressure "pips" could occur whether turbulence originated above or below piezometer No. 2 since the absolute velocity of the upstream interface is greater than that of the downstream interface.

Another indication of the origin of turbulence may be obtained by plotting the hydraulic grade line at successive time intervals. The appearance of a discontinuity in the grade line may be attributed to a turbulent formation. For Run No. 29, this discontinuity seems to appear between piezometers No. 2 and 3 as may be seen in Fig. 3. Therefore the application of Eq. (2) upstream from piezometer No. 3 would yield unreliable results, but it may be safely applied between piezometers Nos. 3 and 4, and 4 and the outlet.

The velocity of the downstream interface V^* could conceivably be a function of the mean velocity V, the pipe radius r_o, the distance from where turbulence started x, the laminar boundary layer thickness δ, and the kinematic viscosity υ.

$$V^* = \phi (V, r_o, \delta, x, \upsilon)$$

In dimensionless form, the functional relationship may be expressed as,

$$\frac{V^*}{V} = \phi \left[\frac{VD}{\upsilon}, \frac{\delta}{r_o}, \frac{x}{D} \right] \qquad (3)$$

The values of V^*/V determined from experimental data were nearly constant at about 1.35. Therefore, the downstream interface moves somewhat faster than the mean velocity V. The constancy of V^*/V is indicative that the movement is independent of the laminar flow preceding the interface and thus V^*/V is independent of the variables on the right side of Eq. (3). The dimensionless relative velocity, $(V^*-V)/V = 0.35$ is indicative of the rate at which the laminar flowing fluid is entrained by the turbulent eddies at the interface. The values of V^*/V are shown on Fig. 9 as a function of the experimental dimensionless parameters.

Point of Turbulence Inception.—The point of inception of turbulence may be estimated by reference to the pressure-time curves or by plotting the hydraulic grade line at sufficiently close successive intervals of time as is explained in the preceeding section. However, by utilizing the calculated time of turbulence inception and the calculated rate of growth of turbulence in the downstream direction, one may arrive at an exact point for the origin of turbulence. The accuracy of this method is obviously dependent upon the accuracy of the calculated time of turbulence inception and the calculated rate of growth of turbulence in the downstream direction.

The conclusion of the preceeding section is that turbulence progreses downstream at a rate of about 1.35 V. If one obtains the time that it takes the laminar-turbulent interface to progress downstream from its unknown point of origin to a point of known location (a piezometer), the distance from the origin to the point of known location may be calculated. Thus

$$\ell^* = V^*(\Delta t) = 1.35V\ (\Delta t) \qquad (4)$$

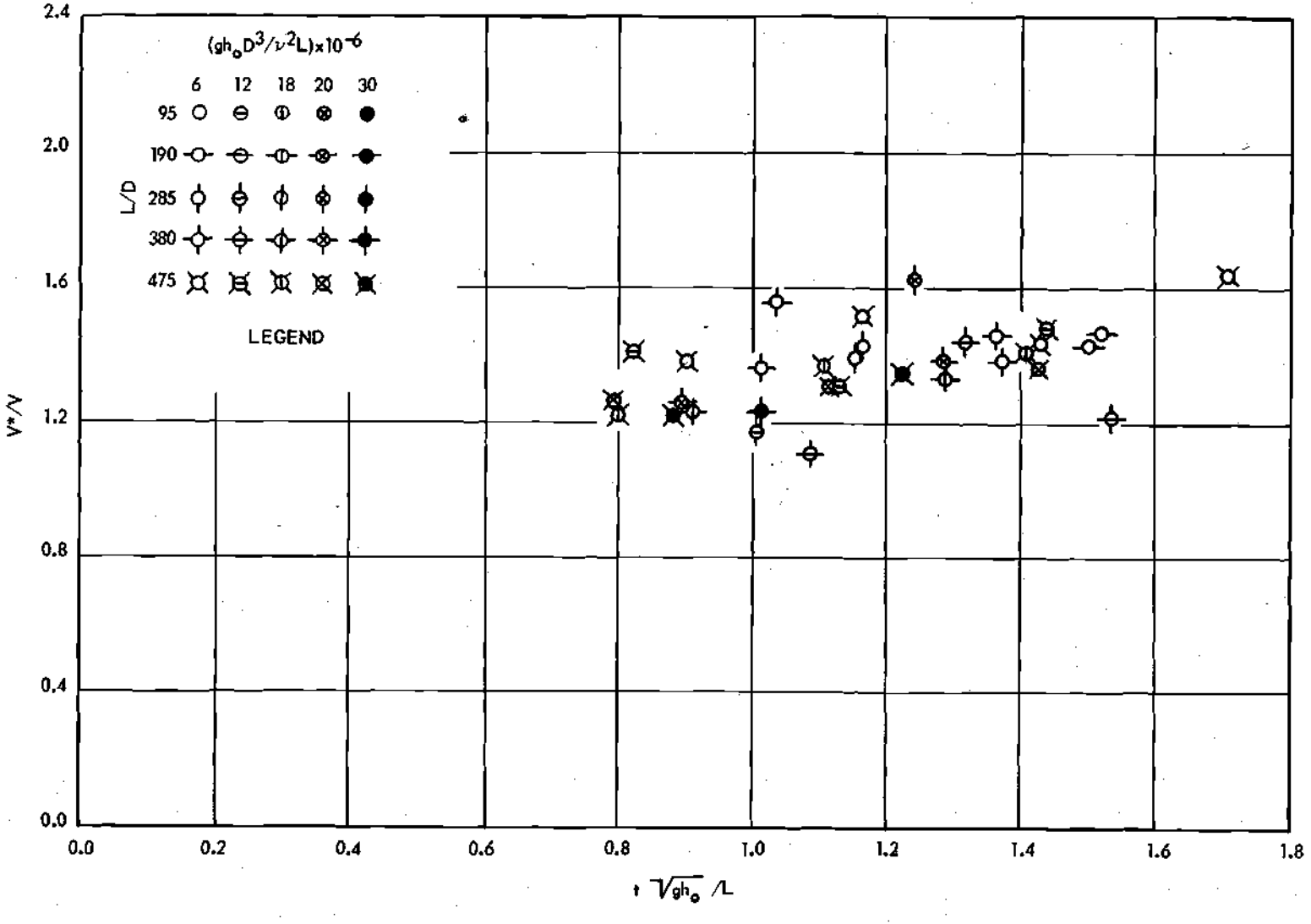

Figure 9. The Dimensionless Downstream Rate of Growth of Turbulence.

where ℓ^* is the distance from the origin of turbulence to the piezometer chosen, and Δt is the difference in the time of turbulence inception and the time that turbulence reaches the piezometer chosen. The distance from the inlet to the point of turbulence inception ℓ'', is equal to the distance from the inlet to the piezometer chosen minus ℓ^*.

Any piezometer downstream from the point of inception may be utilized in this computation. However, it is desirable to use the first piezometer below the point of inception. In this way, because of the smaller interval of time from the time of inception to the time the interface reaches the piezometer, greater accuracy may be obtained in selecting the average V. But since the point of inception is not yet determined, one can not be sure which piezometer should be used. Therefore, one should initially utilize a piezometer that is located sufficiently far downstream for there to be no possibility of turbulence originating below it. If the resulting ℓ^*/D is greater than 95 (the distance to the next upstream piezometer), the next upstream piezometer may be utilized.

The point of turbulence inception as determined in this manner agrees with that predicted by the sequence of occurrence of pressure "pips" in the pressure-time curves. It is also in agreement with that predicted by the appearance of a discontinuity in the hydraulic grade line. For instance, in the preceeding section the point of turbulence inception in Run No. 29 is deduced to be between 94 and 284 pipe diameters from the inlet from the pressure-time curves, and between 189 and 284 pipe diameters from the inlet from the hydraulic grade lines. Equation (4) yields for Run No. 29 a point of turbulence inception 210 pipe diameters from the inlet.

It seems logical that the point at which turbulence originates depends upon the conditions existing at that time and only indirectly upon the history of the motion. That is, the history is significant only in respect to establishing the existing conditions. Thus,

$$\ell'' = \phi(V, D, \nu, \delta)$$

$$\frac{\ell''}{D} = \phi\left[\frac{VD}{\nu}, \frac{\delta}{r_o}\right]$$

These functions were evaluated at the time of turbulence inception and plotted. The resulting figures indicated that ℓ''/D is independent of both R and δ/r_o. Apparently, the point at which turbulence appears is a random point. Schubauer and Klebanoff [6] came to this conclusion after studying flow past a flat plate. However, it is of interest to note that the points of turbulence inception for duplicate runs were very nearly the same ($\pm$ 20) as those for the original runs. Values of ℓ''/D for the original runs are shown in Fig. 10.

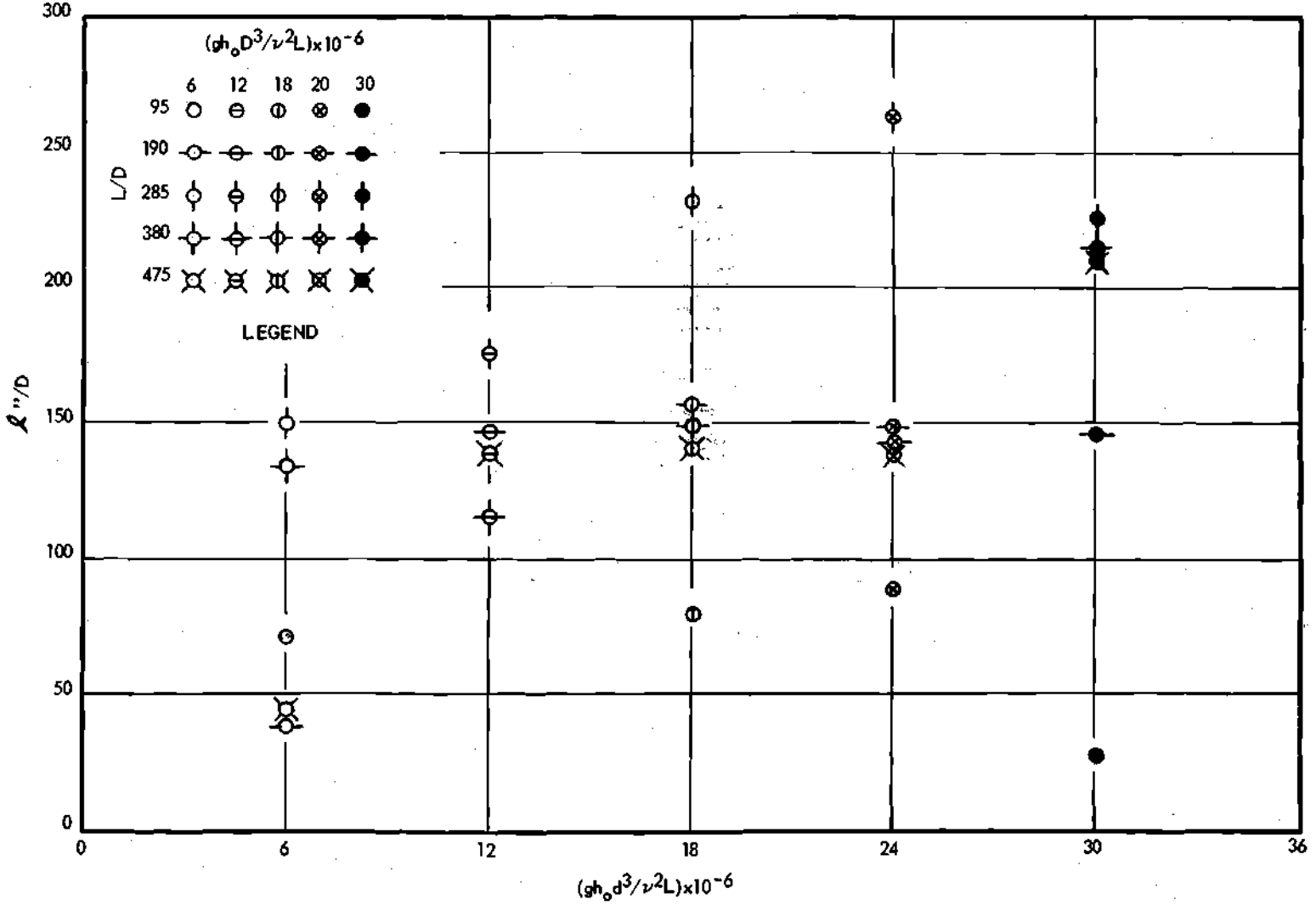

Figure 10. Dimensionless Distance from the Inlet to the Point of Turbulence Inception.

CHAPTER IV

CONCLUSIONS

The following conclusions may be drawn from this study of the laminar-turbulent transition:

(1) The transition from laminar to turbulent flow is the result of boundary layer instability. When R_δ reaches a value of about 5,500, disturbances in the boundary layer are no longer dampened but rather are amplified until they become of such magnitude that laminar motion ceases to exist.

(2) The transition from laminar to turbulent flow does not occur instantaneously throughout the pipe. Turbulence originates at a point and progresses upstream and downstream.

(3) The upstream progression of turbulence is the result of new regions of instability.

(4) The downstream progression of turbulence is the result of transport by the mean velocity of the fluid plus the entrainment of laminar flowing fluid by the turbulent at the laminar-turbulent interface. This entrainment is approximately at a rate equal to 0.35 V.

(5) The point at which turbulence originates is not predictable, but for sufficiently long lengths of pipe, turbulence originates in the upstream region (30 to 270 pipe diameters from the inlet).

REFERENCES

[1]. Prandtl, L. and O. G. Tietjens, Applied Hydro- and Aeromechanics, translated by J. P. Den Hartog, 1st ed. New York and London, McGraw-Hill, 1934, pp. 29-40.

[2]. Dryden, H. L., Some Recent Contributions to the Study of Transition and Turbulent Boundary Layers, Technical Note No. 1168, National Advisory Committee for Aeronautics, April 1947.

[3]. Schlichting, H., Boundary Layer Theory, Technical Memorandum No. 1218 (Part II), (Translation from the German), National Advisory Committee for Aeronautics, April 1949, pp. 74-91.

[4]. Schubauer, G. B., and H. K. Skramstad, "Laminar Boundary-Layer Oscillations and Stability of Laminar Flow", Journal of the Aeronautical Sciences, Vol. 14, No. 2, 1947, p. 69.

[5]. Goldstein, S., Modern Developments in Fluid Dynamics, Vol. I, 1st ed. Oxford University Press, 1938, pp. 319-330.

[6]. Schubauer, G. B., and P. S. Klebanoff, Contributions on the Mechanics of Boundary-Layer Transition, Technical Note 3489, National Advisory Committee for Aeronautics, Sept. 1955.

APPENDIX A

EVALUATION OF THE PIEZOMETRIC HEAD AT THE INLET SECTION

The effect of flow unsteadiness upon the value of the piezometric head in the inlet section of a pipe attached to a large reservior is to be evaluated. The flow into a streamlined inlet of a pipe is presumed to approach this inlet in a manner similar to the three-dimensional hydrodynamic sink (Fig. 1A)

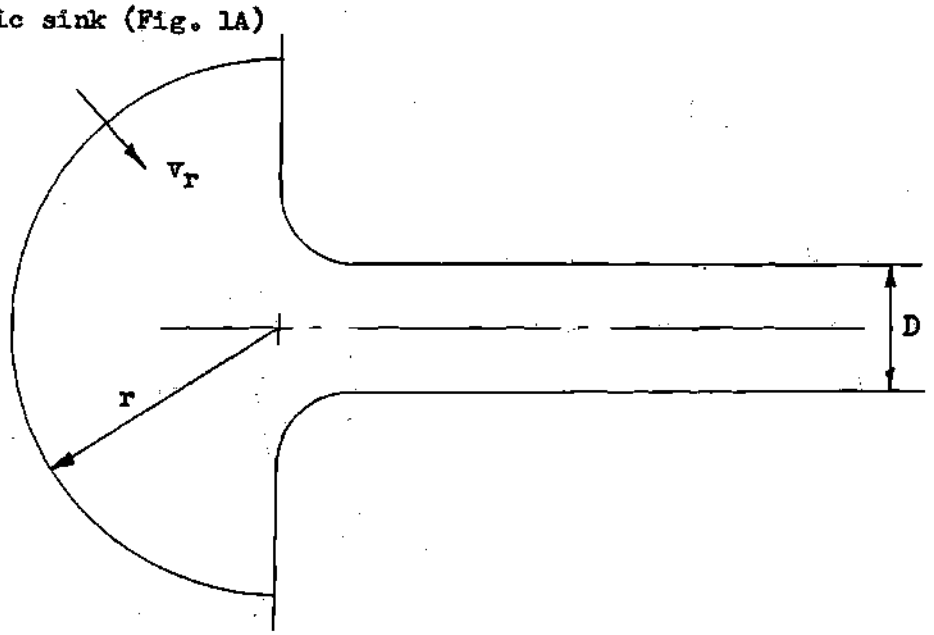

Fig. 1A. Flow into a Streamlined Inlet of a Pipe

The velocity is entirely in the radial direction, the velocity-potential surfaces are hemispherical, and the velocity magnitude is constant on each potential surface. With an incompressible fluid, the volume rate of flow Q past every normal section is a function only of time. Thus the equation of continuity can be written in the following forms,

$$Q = VA = V\frac{D^2\pi}{4} \qquad (1A)$$

and

$$Q = -v_r \, 2\pi r^2 \tag{2A}$$

in which V is the mean velocity in the pipe, D is the pipe diameter, r is radial coordinate of the sink, and v_r is the velocity in the field of the sink. Thus,

$$v_r = -\frac{D^2}{8r^2} V \tag{3A}$$

and

$$\frac{\partial v_r}{\partial t} = -\frac{D^2}{8r^2} \frac{dV}{dt} \tag{4A}$$

Since the shear is negligible in the sink field, the equation of motion is

$$-\frac{\partial p}{\partial r} = \rho v_r \frac{\partial v_r}{\partial r} + \rho \frac{\partial v_r}{\partial t} \tag{5A}$$

in which ρ is the fluid density and p is the piezometric pressure. Substituting Eq. (4A) in Eq. (5A) and taking the dot product with dr, the differential work-energy equation is derived.

$$-\frac{\partial}{\partial r}\left[\frac{\rho v_r^2}{2} + p\right] \cdot dr = \rho \frac{D^2}{8} \frac{dV}{dt} \frac{1}{r^2} \cdot dr \tag{6A}$$

the indicated integration is performed with the following limits; as $r \to \infty$, $v_r \longrightarrow 0$, $p \longrightarrow p_o$ in which p_o is the piezometric pressure in the large reservoir. The lower limit of r is $D/\sqrt{8}$ or the position at which $|v_r| = |V|$. The result is

$$p_1 = p_o - \rho \frac{V^2}{2} - \frac{\rho D}{\sqrt{8}} \frac{dV}{dt} \tag{7A}$$

Dividing by the specific weight γ and the constant reservoir piezometric head h_o,

$$\frac{h_1}{h_o} = 1 - \frac{V^2}{2gh_o} - \frac{D}{\sqrt{8}\, gh_o} \frac{dV}{dt} \tag{8A}$$

The entire effect of unsteadiness of the motion is expressed in the third term on the right side of the equation.

APPENDIX B

ONE-DIMENSIONAL EQUATION OF PIPE FLOW

Unsteady flow in a smooth pipe is a flow situation to which the method of one-dimensional analysis can be advantageously utilized. The advantage of this method is that the equation of motion is for the total fluid cross section.

The two fundamental concepts of one-dimensional analysis are as follows: (1) the piezometric pressure or piezometric head is constant in a cross section which is normal to the direction of flow; and (2) the various point velocities can be replaced by the mean velocity V of the cross section. The first concept is satisfied in the straight pipe except in a very short region following the inlet where the flow is definitely non-uniform. Slight nonuniformity of the flow as in the spatially growing boundary layer is of little effect on the piezometric head constancy across the pipe. The second concept concerning the use of the mean velocity is directly applicable in the equation of continuity for the total cross section. However, in order to utilize the mean velocity in the momentum equation, the linear momentum flux must be multiplied by the momentum correction coefficient K_m in order to obtain the true linear momentum flux.

The fluid element used in the derivation is an element dx in length with a cross sectional area equal to the pipe as shown on Fig. 1B.

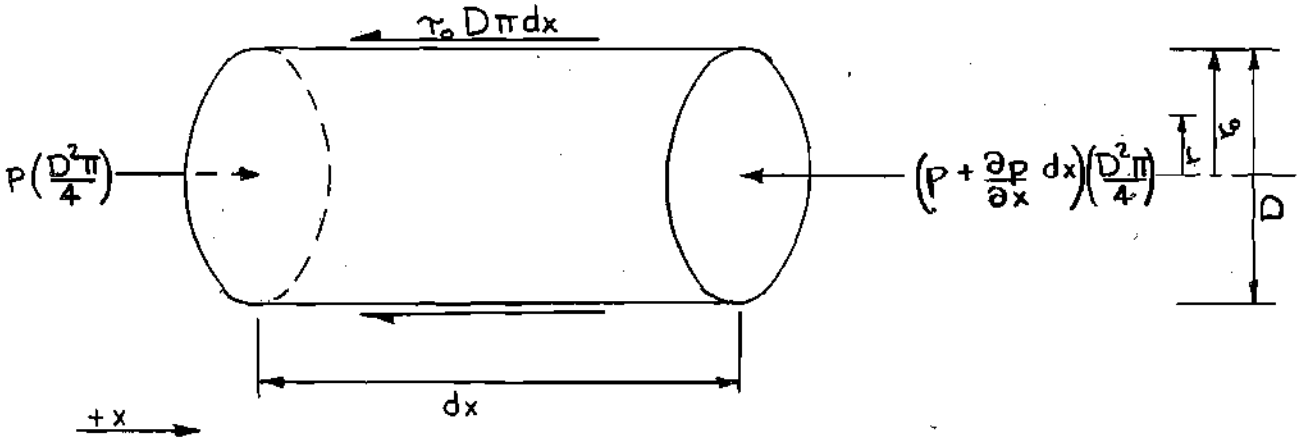

Fig. 1B. Fluid Element within the Pipe

The external forces on the fluid element in the x direction are the resultant pressure force on the end areas and the boundary shear force. The momentum equation for this element is

$$-\frac{\partial p}{\partial x} dx \frac{D^2\pi}{4} - \tau_o D\pi dx = \frac{\partial}{\partial x}\left[\int^A \rho v \, dQ\right] dx + \frac{\partial}{\partial t} \int^{\forall} \rho v \, d\forall \quad (1B)$$

in which τ_o is the boundary shear stress and $\forall$ is the volume of the fluid element. The first term on right side of Eq. (1B) is the difference of momentum flux through the end areas of the fluid element. Utilizing the one-dimensional method of writing momentum flux

$$\int^A \rho v \, dQ = K_m \rho QV = K_m \rho V^2 \frac{D^2\pi}{4} \quad (2B)$$

in which K_m is the linear momentum correction coefficient. The second term on the right side of Eq. (1B) is the time rate of change of linear momentum of the particles on the interior of the element. The incremental volume $d\forall$ is

$$d\forall = dA \, dx$$

The end areas of the element are chosen such that dx is a constant for every dA. Thus,

$$\frac{\partial}{\partial t} \int_{\forall} \rho v \, d\forall = \frac{\partial}{\partial t} \left[\int_{A} \rho v \, dA \right] dx = \rho \frac{\partial Q}{\partial t} dx \tag{3B}$$

Since

$$Q = VA$$

and since Q is a function of time alone

$$\frac{\partial Q}{\partial t} = \frac{D^2 \pi}{4} \frac{dV}{dt} \tag{4B}$$

Introducing Eqs. (2B), (3B), and (4B) into Eq. (1B) and expressing the result on a unit volume basis, the one-dimensional equation of motion is

$$- \frac{\partial p}{\partial x} - \frac{4 \tau_o}{D} = \rho V^2 \frac{\partial K_m}{\partial x} + \rho \frac{dV}{dt} \tag{5B}$$

In order to obtain a clearer interpretation of Fig. (4) in relationship to the equation of motion, Eq. (5B) is transformed into dimensionless form by dividing by h_o and γ, and multiplying by D.

$$- \frac{\partial (h/h_o)}{\partial (x/D)} - \frac{4 \tau_o}{\gamma h_o} = \frac{V^2}{g h_o} \frac{\partial K_m}{\partial (x/D)} + \frac{D}{g h_o} \frac{dV}{dt} \tag{6B}$$

The physical interpretation of the various terms of Eq. (6B) are as follows. The first term on the left side is the dimensionless motivating force of the motion. This motivating force is the slope of the dimensionless curves, h/h_o versus x/D, shown on Fig. 4. The second term on the left is the dimensionless shear force which always acts so as to oppose the motion. For purposes of qualitative analysis this shear force can

be considered to be proportional to V in laminar flow and to be proportional to V^2 in turbulent flow. The first term on the right is the change of momentum flux with respect to distance. Since the value of the momentum correction coefficient K_m is dependent only upon velocity distribution, $\partial K_m / \partial (x/D)$ will be zero in the region sufficiently distant from the inlet. The region in which $\partial K_m / \partial (x/D)$ is not zero is known as the inlet length. The second term on the right side of Eq. (6B) is the change of linear momentum with respect to time alone and thus is the same value throughout the pipe at a given instant.

For flow establishment in a straight pipe with a well-rounded inlet, certain facts can be deduced from Eq. (6B). In the region downstream from the inlet length or where $\partial K_m / \partial (x/D) = 0$, these deductions are as follows:

a. The effect of a positive value of acceleration dV/dt on the piezometric head gradient is the same as that of shear. In other words, the piezometric head gradient is greater than that due to shear alone.

b. The effect of a negative value of acceleration dV/dt on the piezometric head gradient is opposite to that of shear. In other words, the piezometric head gradient is less than that due to shear with negative acceleration. In fact, if the deceleration is sufficiently great the piezometric head can increase in the direction of flow even though the effect of shear is always to cause a decreasing piezometric head in the direction of flow.

c. The piezometric head line is a straight line at a given instant. In the region downstream from the inlet region the velocity distribution is not changing with respect to distance, therefore the shear force would be independent of distance as is dV/dt. Therefore the piezometric head gradient is a constant with respect to distance in this region.

In the region of the inlet length or where $\partial K_m / \partial (x/D) \neq 0$, these deductions are as follows:

d. $\partial K_m / \partial (x/D)$ is always positive in this region with the result the piezometric head gradient is greater than that due to shear alone. $\partial K_m / \partial (x/D)$ must be positive in this region as K_m has a minimum value of unity at the inlet and increases as the velocity profile is developed with distance. Consequently, the piezometric head gradient is steeper in the inlet length than in a region further downstream.

e. The piezometric head line is a curved line at a given instant. K_m is a minimum at the inlet and increases with distance. However, the greatest change in the value of K_m occurs near the inlet. Therefore the piezometric head line is a curved line which is concave upward in the inlet length.

APPENDIX C

TABULATED EXPERIMENTAL VALUES AT THE TIME TURBULENCE WAS FIRST OBSERVED

Run No.	$\frac{gh_o D^3}{\upsilon^2 L}(10^{-6})$	L/D	Distance to the point of observation from the inlet in D's	$t\sqrt{gh_o}/L$ At the time of turbulent passage	$\frac{V}{\sqrt{2gh_o}}$ At the time of turbulent passage
8	6.03	95	95	1.78	0.535
7	12.0	95	95	1.21	0.535
6	18.1	95	95	1.31	0.545
5	24.0	95	95	1.11	0.535
4	30.2	95	95	1.73	0.575
10(3)	5.99	190	94	1.22	0.458
10(3)	5.99	190	190	1.70	0.432
10a	6.00	190	94	1.23	0.458
9	12.0	190	94	1.22	0.480
9	12.0	190	190	1.22	0.480
9(2)	12.0	190	94	1.08	0.453
9(2)	12.0	190	190	1.08	0.453
11	17.9	190	94	1.18	0.462
11	17.9	190	190	0.990	0.445
11a	18.0	190	94	1.10	0.461
11b	17.9	190	94	1.11	0.461
12	23.9	190	94	1.19	0.455
12	23.9	190	190	1.00	0.449
12b	24.1	190	94	0.884	0.433
13	29.9	190	94	1.17	0.452
13	29.9	190	190	0.980	0.445
13a	29.9	190	94	1.15	0.452
13b	30.0	190	94	0.740	0.399
15	5.98	285	94	0.985	0.385
15	5.98	285	189	0.937	0.384
15	5.98	285	285	1.32	0.360
16	12.0	285	94	0.672	0.341
16	12.0	285	285	1.24	0.357
16a	12.0	285	94	0.680	0.344
16a	12.0	285	189	0.724	0.353
17	18.0	285	94	0.659	0.338
17	18.0	285	189	0.678	0.341

(Continued)

Run No.	$\frac{gh_o D^3}{\nu^2 L}(10^{-6})$	L/D	Distance to the point of observation from the inlet in D's	$t\sqrt{gh_o}/L$ At the time of turbulent passage	$\frac{V}{\sqrt{2gh_o}}$ At the time of turbulent passage
17	18.0	285	285	0.892	0.359
18	24.0	285	94	0.608	0.318
18	24.0	285	189	0.624	0.322
18	24.0	285	285	0.703	0.334
19	30.0	285	94	0.606	0.325
19	30.0	285	189	0.682	0.342
19	30.0	285	285	0.879	0.359
20	5.99	380	94	0.801	0.359
20	5.99	380	189	0.880	0.364
20	5.99	380	380	1.53	0.325
20a	5.98	380	189	0.831	0.362
20a	5.98	380	284	1.19	0.360
20b	5.96	380	189	0.837	0.362
20b	5.96	380	284	1.19	0.360
21	12.0	380	94	0.817	0.364
21	12.0	380	284	1.14	0.357
21	12.0	380	380	1.45	0.325
21a	12.0	380	189	0.864	0.368
21a	12.0	380	284	1.31	0.345
22	18.0	380	94	0.789	0.365
22	18.0	380	284	1.10	0.365
22	18.0	380	380	1.44	0.335
22a	17.9	380	94	0.551	0.302
22a	17.9	380	189	0.714	0.352
23	23.9	380	94	0.730	0.348
23	23.9	380	284	1.09	0.364
23	23.9	380	380	1.43	0.342
23a	24.0	380	94	0.585	0.317
23a	24.0	380	189	0.702	0.345
23b	24.0	380	94	0.737	0.350
23b	24.0	380	284	1.10	0.363
24	30.3	380	94	0.658	0.332
24	30.3	380	284	0.803	0.351
24	30.3	380	380	1.18	0.340
24a	29.9	380	94	0.642	0.328
24a	29.9	380	189	0.690	0.338
25	5.98	475	94	0.761	0.343
25	5.98	475	284	1.29	0.359
25	5.98	475	475	1.80	0.292
25a	5.97	475	189	1.04	0.371
25a	5.97	475	379	1.57	0.327

(Continued)

Run No.	$\frac{gh_o D^3}{\upsilon^2 L}(10^{-6})$	L/D	Distance to the point of observation from the inlet in D's	$t\sqrt{gh_o}/L$ At the time of turbulent passage	$\frac{V}{\sqrt{2gh_o}}$ At the time of turbulent passage
26	12.0	475	94	0.716	0.331
26	12.0	475	284	0.971	0.341
26	12.0	475	475	1.53	0.325
26a	12.0	475	189	0.676	0.325
26a	12.0	475	379	1.29	0.327
27	18.0	475	94	0.702	0.331
27	18.0	475	284	0.964	0.344
27	18.0	475	475	1.53	0.310
27a	18.0	475	94	0.696	0.330
27a	18.0	475	284	0.959	0.344
27b	18.0	475	189	0.624	0.315
27b	18.0	475	379	1.26	0.330
27c	18.0	475	189	0.622	0.314
27c	18.0	475	379	1.26	0.330
27d	17.9	475	189	0.641	0.318
27d	17.9	475	379	1.27	0.328
27e	17.9	475	189	0.626	0.315
27e	17.9	475	379	1.26	0.330
27f	17.9	475	189	0.638	0.317
27f	17.9	475	379	1.26	0.330
28	23.9	475	94	0.655	0.322
28	23.9	475	284	0.959	0.348
28	23.9	475	475	1.54	0.310
28a	24.0	475	189	0.628	0.316
28a	24.0	475	379	1.27	0.336
29	29.9	475	94	0.650	0.318
29	29.9	475	284	0.715	0.327
29	29.9	475	475	1.33	0.306
29a	30.0	475	189	0.616	0.312
29a	30.0	475	379	1.06	0.327